

How to determine the permeability for cement infiltration of osteoporotic cancellous bone

G. Baroud ^{a,*}, J.Z. Wu ^b, M. Bohner ^c, S. Sponagel ^d, T. Steffen ^a

^a McGill University, Orthopaedic Research Laboratory, Royal Victoria Hospital, 687 Pine Avenue West, Montreal, QC H3A 1A1, Canada

^b National Institute for Occupational Safety & Health, Morgantown, West Virginia 26505, USA

^c Dr. H. C. Robert Mathys Foundation, 2544 Bettlach, Switzerland

^d University of Applied Science of Aachen (FH), Biomedical Engineering, Jülich, Germany

Abstract

Cement augmentation is an emerging surgical procedure in which bone cement is used to infiltrate and reinforce osteoporotic vertebrae. Although this infiltration procedure has been widely applied, it is performed empirically and little is known about the flow characteristics of cement during the injection process. We present a theoretical and experimental approach to investigate the intertrabecular bone permeability during the infiltration procedure. The cement permeability was considered to be dependent on time, bone porosity, and cement viscosity in our analysis. In order to determine the time-dependent permeability, ten cancellous bone cores were harvested from osteoporotic vertebrae, infiltrated with acrylic cement at a constant flow rate, and the pressure drop across the cores during the infiltration was measured. The viscosity dependence of the permeability was determined based on published experimental data. The theoretical model for the permeability as a function of bone porosity and time was then fit to the testing data. Our findings suggest that the intertrabecular bone permeability depends strongly on time. For instance, the initial permeability ($60.89 \text{ mm}^4/\text{N}\cdot\text{s}$) reduced to approximately 63% of its original value within 18 seconds. This study is the first to analyze cement flow through osteoporotic bone. The theoretical and experimental models provided in this paper are generic. Thus, they can be used to systematically study and optimize the infiltration process for clinical practice.

Keywords: Cement infiltration; Vertebroplasty; Osteoporosis; Permeability; Experiment; Analysis; Viscous flow

1. Introduction

The prevalence of osteoporotic fractures increases rapidly with aging. In the USA alone, osteoporosis is responsible for 1.5 million fractures annually with 700,000 being predominantly vertebral compression fractures (VCF) [1]. As life expectancy increases, the financial pressures on health care systems are growing dramatically. Already, the total annual cost of all osteoporosis-related fractures is at least \$5–\$10 billion [1]. Current treatment for VCF is bed rest and pain medication. Surgical treatment of osteoporosis is unsatisfactory because conventional internal fixation systems (e.g.,

screws, rods) fail to adequately anchor in osteopenic bone.

Vertebroplasty is an emerging surgical procedure to reinforce the bone structure of osteoporotic vertebrae by filling the porous cancellous bone with bone cement. This procedure is increasingly used in Europe and North America for the treatment of patients suffering vertebral compression fractures due to osteoporosis [2–4]. Many studies reported that this procedure provides significant and rapid pain relief in 80–90% of patients [2,3,5]. The long-term safety and efficacy of this procedure still remain to be proven.

Since the cement augmentation procedure is still on the experimental level, the injection procedure is not yet standardized. Inadequate injection may lead to adverse complications. For instance, if the cement is injected while too liquid, it may spread quickly throughout the trabecular cavities, in an uncontrolled manner, and result

* Corresponding author. Tel.: +1-514-842-1231 ext. 35274; fax: +1-514-843-1699.

E-mail address: gbaroud@orl.mcgill.ca (G. Baroud).

in leakage. However, if it is injected while too viscous, the pressure required for injection becomes high, resulting in poor filling because the surgeon is not able to build enough pressure to force the cement to infiltrate the trabeculae. In order to optimize the injection parameters of the procedure, we need to understand the fluid dynamics of cement infiltration into osteoporotic cancellous bone. To the authors' knowledge, there exist no reports on the analysis of cement infiltration into the cancellous structure of osteoporotic bone.

Bone cements are typically obtained as a two-component system. After mixing the two components, the viscosity coefficient rapidly increases with time. A catalyst, usually present in the powder, initiates the curing. The cement is injected into the anterior aspect of the vertebral body while it is liquid. The cement gradually displaces the bone marrow until it fills the trabecular cavities.

The hydraulic permeability of the bone, while injecting the cement, depends on bone porosity and changing cement viscosity, which is time and shear-rate dependent [6]. A better understanding of bone permeability will help to optimize the injection parameters (e.g., pressure, volume, cement viscosity), making the infiltration process predictable and reproducible. The purpose of this study was to investigate, theoretically and experimentally, the permeability of cancellous bone with respect to time and porosity.

2. Methods

2.1. Permeability analysis

The cement is a thick viscous fluid, that exhibits a shear thinning behavior [6]. The cement flow in permeable bone is slow. Thus, it can be approximated using Darcy's law:

$$v = \kappa \frac{\partial p}{\partial x} \quad (1)$$

where v is the infiltration rate, $\partial p/\partial x$ is the pressure gradient, and κ is the intertrabecular bone permeability.

For the cement infiltration procedure, κ is generally a function of the intertrabecular bone porosity, α , and cement viscosity, η :

$$\kappa = \kappa(\alpha, \eta) \quad (2)$$

The permeability is measured using a test set-up shown in Fig. 1. The average pressure gradient across the specimen, $\partial p/\partial x$, and the infiltration speed, v , are to be determined from the experiment; and the bone permeability, κ , is to be calculated using Eq. (1). In order to determine the pressure gradient across the specimen, $\partial p/\partial x$, the force balance is analyzed as shown in the free body diagram (Fig. 2).

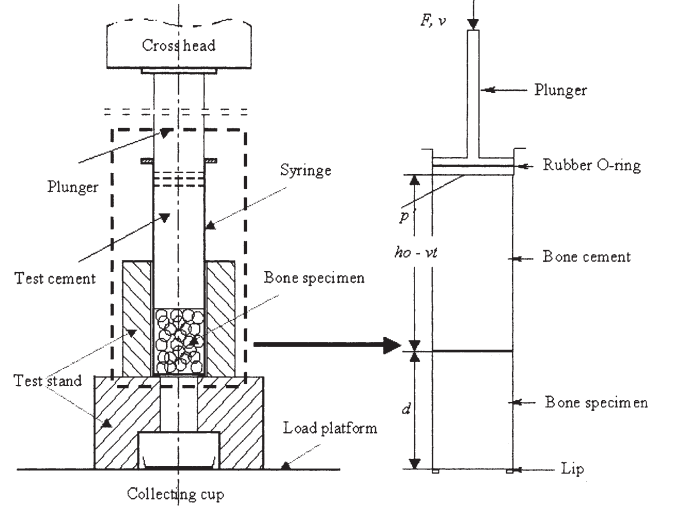


Fig. 1. Experimental set-up for the determination of permeability of cancellous bone. A cancellous bone core (diameter = 14.4 mm, height (d) = 14 mm) was placed at the bottom of a 15 cc syringe. Cement was poured into the syringe, levelled to the upper rim. The initial height of the cement column, h_0 was approximately 40 mm. Using the MTS testing machine, the plunger was pressed down at a constant injection speed, v , of 2 mm/s, forcing the cement to flow through the interstitial space of the cancellous bone and reducing the height of the cement column by $h_0 - vt$. The pressure, $p' = F/A$, in response to the linear injection of 2 mm/s was recorded over the course of the experiment.

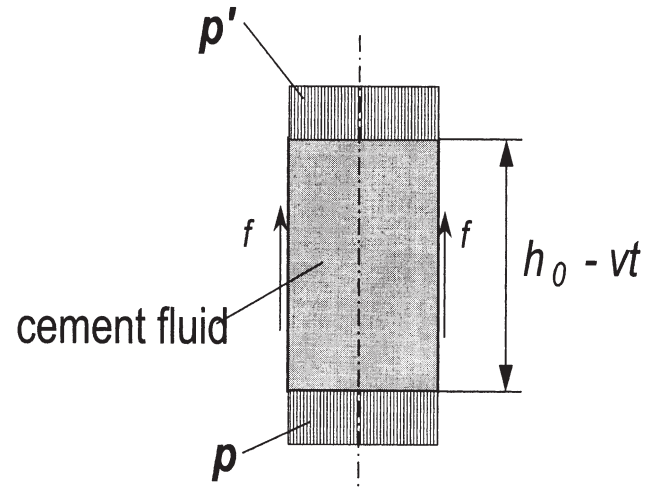


Fig. 2. Force balance of the liquid cement. The pressure acting at the upper interface of the bone specimen, p , is in equilibrium with the plunger pressure, p' , and the wall frictional surface forces, f , of the tube wall.

The pressure response at injection, p' , is balanced by the pressure at the interface between the cement and bone, p , and the friction between the cement and wall, f :

$$p' \pi r^2 = p \pi r^2 + f = p \pi r^2 + \beta \int_0^h 2 \pi r \eta dy \quad (3)$$

where r is the tube radius, p' is the pressure measured

at the plunger tip and is related to the injection force, F , by $p' = F/\pi r^2$; h is the height of the fluid cement column. It is assumed here that the friction between the cement and wall, f , is induced by the viscous adhesiveness of the fluid cement to the wall and is proportional to the injection speed, v , and cement viscosity, η , which is usually dependent on shear rate γ and time, i.e., $\eta = \eta(\gamma, t)$ with γ and t being the shear rate and time, respectively. β is the friction coefficient between the fluid and the syringe wall, which is associated with the surface characteristics of the syringe wall; for thick viscous fluid like cement, $\beta \approx 1$.

Assuming that the injection speed is constant at v and the height of liquid is originally h_0 at $t = 0$, and the shear is uniformly distributed along the height of the tube wall, Eq. (3) is then expressed as:

$$p(t) = p'(t) - \frac{2}{r}\beta(h_0 - vt)\gamma\eta(t, \gamma) \quad (4)$$

Using Darcy's law, Eq. (1), the permeability of the bone core can be determined as follows:

$$\kappa(t) = \frac{v}{(p - p_0)/d} = \frac{vd}{p'(t) - \frac{2}{r}(h_0 - vt)\gamma\eta(t, \gamma)} \quad (5)$$

where d is the height of the bone core, and $p_0 = 0$ is the atmospheric pressure.

In order to determine the time-dependent permeability, the cement viscosity has to be a priori known. The viscosity of the cement typically depends on time and shear rate in an over-proportional fashion [7], and thus it can be described by a power law commonly used in polymer engineering:

$$\eta = \left[a \left(\frac{t}{t_s} \right) + b \right] \cdot \left(\frac{\gamma}{\gamma_s} \right)^{-c \left(\frac{t}{t_s} \right) + d} \quad (6)$$

where $t_s = 1.0$ min and $\gamma_s = 1.0$ 1/s are a characteristic time and shear rate, respectively; a , b , c , and d are viscosity material parameters, which are to be determined by fitting Eq. (6) to the viscosity test data.

2.2. Permeability measurements

We conducted ten uniform infiltration experiments on isolated cores of osteoporotic bone, using a custom-built infiltration device shown in Fig. 1. The bone cores, tightly sized to fit, were placed at the bottom of a 15 cc syringe. Bone cement (Simplex, Howmedica, London, UK) was prepared according to the manufacturer's instructions and, immediately after it liquified, poured into the 15 cc syringe, and levelled to the upper rim. A plunger with a stiff tip was inserted into the syringe. Vents were made near the upper rim of the syringe to avoid trapping air between the plunger and the cement during injection. Using a material testing machine (Mini

Bionix 856, MTS, Eden Prairie, MN), the plunger was pressed down at a constant injection speed, v , of 2 mm/s, forcing the cement to flow through the interstitial space of the cancellous bone. Pressure-time curves were recorded. All infiltration tests were performed approximately two and half minutes after the start of the mixing.

2.3. Bone specimen for the identification of bone permeability

Lumbar spines were harvested in the autopsy room from human cadaveric spines (two male donors, age: 58 and 69 years) and their bone mineral density (BMD) was measured using a DEXA scanner (Lunar DPX-L, Lunar Radiation Corporation, Madison, WI). Spines used in this project were osteoporotic (the BMDs of all lumbar vertebrae, used in this study, were below two standard deviations (0.20 g/cm²) of the population mean (0.22 g/cm²) [8]. Two cylindrical core samples were cut from each vertebra by drilling (perpendicular to the endplates) into the left and right portions of the vertebral body. A diamond drill with an inner diameter of 14.4 mm was used for this purpose. These 20 cylindrical specimen were subsequently trimmed to a height of 14 mm, measured with calipers and weighed. Ten samples, taken from the right hemi-vertebra, were infiltrated with cement for the permeability study. The remaining samples were used to examine the elastic parameters of the cores. Before cement infiltration, all specimen (sealed in plastic bags) were conditioned for at least 2 hours in a 37 °C water bath. Thereafter, the testing was conducted at room temperature (22 °C).

2.4. Permeability measurement validation

Because of the complicated non-Newtonian behavior of bone cements, we conducted the validation tests using a linear silicone oil (Viscosity standard 100,000, Brookfield Engineering, Middleboro, MA) of a viscosity similar to bone cement. The silicone oil viscosity was 95 Pa*s and it was not sensitive to changes temperature.

Before testing, the linear relation between the pressure gradient and the infiltration speed (i.e., the suitability of Darcy's law for this investigation) was verified. Using a dedicated bone core, independent infiltration tests were then conducted at speeds of 1, 5, 10, and 20 mm/s. Infiltration at each speed was conducted four times. Based on coefficient of variation, permeability measurements were repeatable within 4%.

Also, the reliability of the experimental procedure to measure the permeability of the brass tube (tube length/tube diameter=20), whose permeability can be analytically calculated based on the Hagen-Poiseuille Law, was examined using the same silicone oil. It was found that the reliability of the experiment was within 5%.

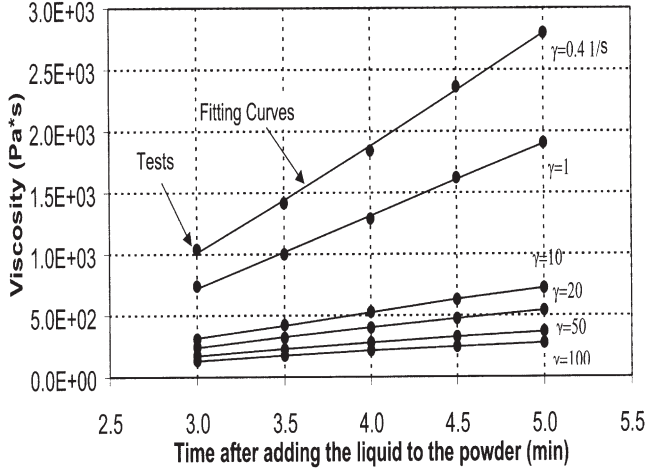


Fig. 3. Comparison of the constitutive equation (Eq. (6)) to experimental data published by Krause [6]. The fitting for the change in cement viscosity with respect to time is presented for six different shear rates. Each line in this figure represents the viscosity increase with time for one shear rate. The viscosity parameters with respect to time, Eq. (6), were found to be $a = 590.0 \text{ Pa*s}$, $b = -1048.8 \text{ Pa*s}$.

3. Results

3.1. Viscosity fitting

Using the viscosity experimental data [6], the viscosity material parameters of Eq. (6) were identified using a least square fit. Eq. (6) provided an accurate fit to the experimental data with respect to time and shear rate, as depicted in Figs. 3 and 4. The viscosity material parameters (Eq. (6)) were found to be $a = 590.0 \text{ Pa*s}$, $b = -1048.8 \text{ Pa*s}$, $c = 0.026$, and $d = 0.290$.

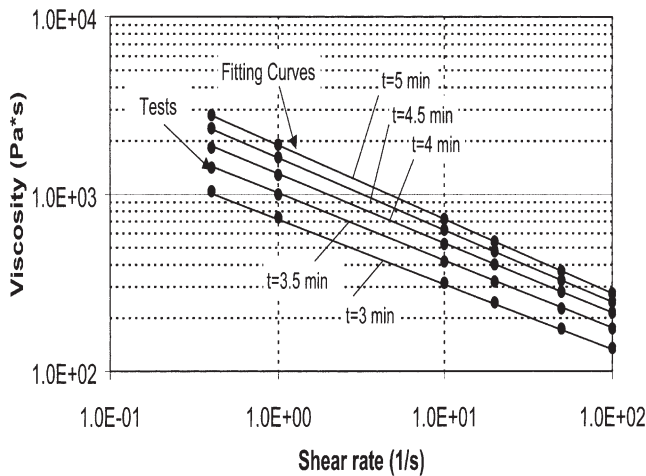


Fig. 4. Comparison of the constitutive equation (Eq. (6)) to experimental data published by Krause [6]. The fitting for the viscosity change with respect to shear rate is represented for five different isochrones (cross point of Fig. 3). Each line (isochrone) represents a change in viscosity only as function of shear rate. The viscosity parameters with respect to time, Eq. (6), were found to be $c = 0.026$, $d = 0.290$.

3.2. Bone permeability

On average, 8 cc of liquid cement was pressed through each specimen, displacing the fat and blood within the interstitial space. Fig. 5 depicts the average pressure-time curve calculated from the ten trials. Using the coefficient of variation, the average variability of the ten pressure-time curves was approximately 32%. All pressure-time curves featured two distinct semilinear regions. The transition point marked the point at which all interstitial bone fluid was displaced and the cancellous bone cavities were completely saturated with bone cement. The first slope represents the increase in pressure needed because of the growing penetration depth of the cement into the specimen. The pressure increase following the transition point occurred because of the decreasing permeability of the specimen, which resulted from the increasing cement viscosity due to the on-going cement polymerization during the infiltration experiment. A line was fitted to the second region of the curve to determine the pressure increase according to Eq. (4). The transition from the first to second region occurred, on average, after injecting 2.08 cc. The average porosity (fluid-volume fraction) was therefore 90.5%, with a range of 87.3 to 96.5%.

The hydraulic permeability, κ , (Eq. (5)) of the cement penetrating the bone cores was determined, as illustrated in Fig. 6. It can be seen that the permeability is strongly dependent on time (1st term of Eq. (4)), while the effect of the tube wall is not relevant (2nd term of Eq. (4)). The wall effect can therefore be ignored for future experiments of similar geometrical set-up.

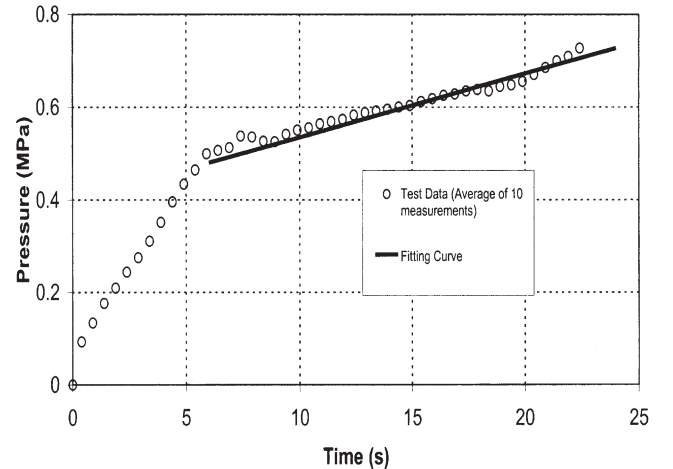


Fig. 5. The average injection pressure with respect to time. All experiments started at approximately two and half minutes after the cement mixing. The first section of the curve represented an increase in the pressure gradient in response to the increased cement penetration into the samples. The increase of the pressure with respect to time after saturation occurred because of increased cement viscosity during testing. A line was fitted to the second section of the curve to quantify the pressure increase because of the increasing cement viscosity.

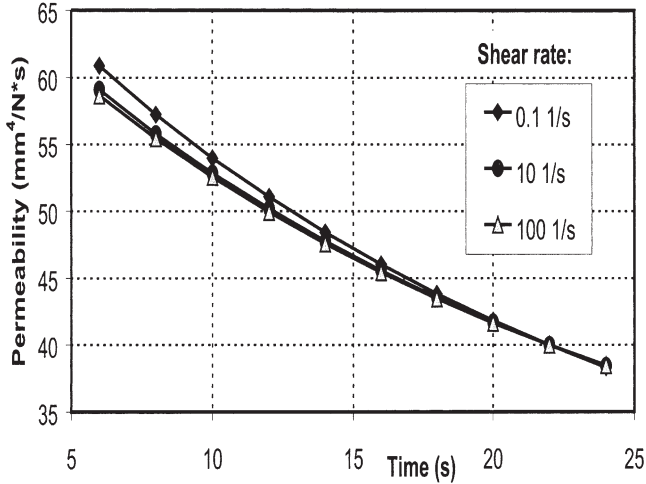


Fig. 6. Time-dependent permeability with respect to time after saturation (second section of the infiltration curve as depicted in Fig. 5). The permeability decreased to approximately 60% of its initial value within approximately 20 s. The three curves in this figure show the effect of the tube wall on permeability (second term of Eq. (4)). The similarity of the three curves shows that the effect of the tube wall is insignificant for the measured permeability.

3.3. Porosity-dependence

The porosity-dependence of the bone permeability can be approximated by [7]:

$$\kappa^*(\alpha) = A \frac{\alpha}{\alpha - 1} \quad (7)$$

where α is the bone porosity and A is a phenomenological parameter.

By fitting Eq. (7) to published data [9,10], the porosity parameter, A , was found to be $0.9 \text{ mm}^4/\text{Ns}$. Fig. 7 shows the comparison of Eq. (7) to the test data.

All our permeability tests were conducted using bone specimens with a porosity approximately $\alpha_0 = 0.90$. In

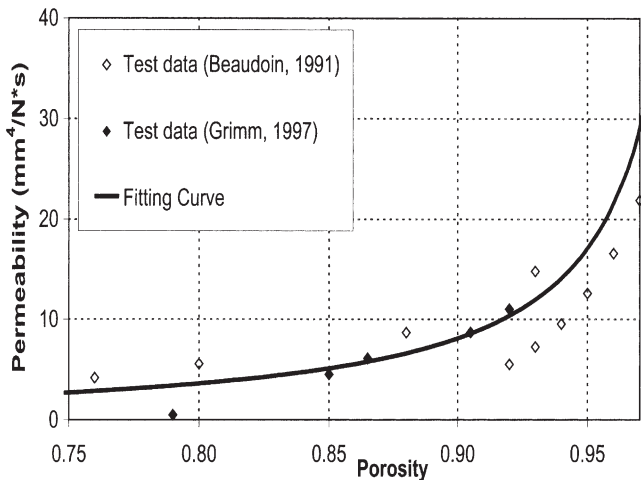


Fig. 7. Fitting the $\kappa_1 = A\alpha(\alpha - 1)$ to the experimental data [9,10]. The parameter used in this fitting was $A = 0.9 \text{ mm}^4/\text{Ns}$.

order to speculate the changes of the permeability due to the variations of the bone porosity, we normalize κ^* to its value at $\alpha_0 (= 0.9)$, i.e., $\kappa_1(\alpha) = \kappa^*(\alpha) / \kappa^*(\alpha_0)$, such that the influence of the bone porosity can be generally accounted by rewriting Eq. (2) into:

$$\kappa = \kappa_1(\alpha)\kappa_2(\eta) \quad (8)$$

where $\kappa_1(\alpha)$ is the permeability as a function of the bone porosity which is normalized to its value of α_0 , and $\kappa_2(\eta)$ is the permeability of the bone specimen with respect to the viscosity η .

The normalized permeability, κ_1 , is plotted as a function of bone porosity in Fig. 8. It is seen that bone permeability increases with increasing porosity, and at $\alpha = \alpha_0 = 0.9$, $\kappa_1 = 1$.

4. Discussion and conclusion

Infiltrating osteoporotic bone with acrylic cements has been recently introduced as an effective treatment for the stabilization of osteoporotic vertebrae. At this time, the infiltration surgery is not standardized and often lacks sophistication or appropriate instruments. The lack of understanding of the bone permeability and the predictability of the cement spread often leads to intraoperative complications. Cement leakage in adjacent structures or blood vessels is the most frequent intraoperative complication, which occurs in as many as 43% of patients [11]. As a result of leakage, the surgery is often interrupted. The injectability of osteoporotic vertebrae is not only unpredictable but sometimes quite difficult. Injection is often interrupted at an early stage because the surgeon is not able to build enough pressure to force the cement to infiltrate the trabeculae. At this point, it is unclear why some vertebrae are not injectable despite similar osteoporotic conditions. Future research will also

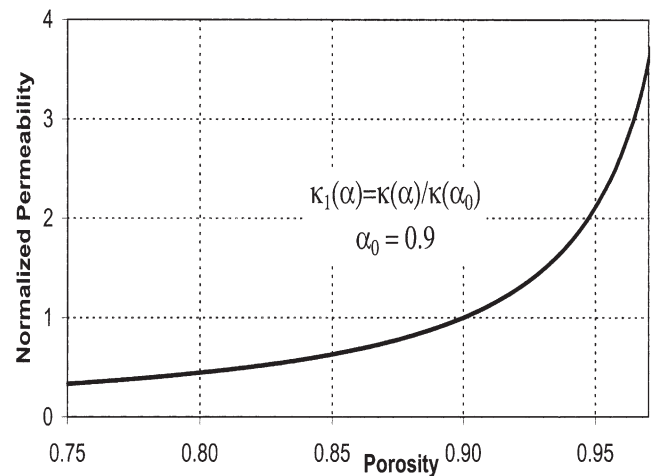


Fig. 8. Normalized permeability as a function of intertrabecular bone porosity. For $\alpha < 0.9$, $\kappa < 1$, while $\kappa > 1$ for $\alpha > 0.9$.

have to investigate optimal cement strategies, making this procedure reliable and reproducible. For this purpose, a mechanistic understanding of cement-spread pattern as a function of cement viscosity and bone porosity is required.

The focus of this paper was to investigate, experimentally and theoretically, the intertrabecular permeability of osteoporotic bone for the infiltration procedure. We assume a slow cement flow and a small deformation of the bone, which are typical to cement injection into bone. We measured the intertrabecular permeability of human vertebrae for one bone cement and one anatomical direction, using a linear flow protocol.

The use of homogeneous (uniform) flow is appealing for the permeability identification because the mathematical treatment is straightforward. We determined the bone permeability in only one direction, assuming the permeability is uniform and isotropic with the cement. We assumed the existence of a macroscopic range in that trabecular bone can be treated as homogeneous and isotropic tissue. In reality, the bone voids are not uniformly distributed within the bone. The assumption of homogeneity is mandatory, but that of isotropy is a convenient simplification. The anisotropy can be simply introduced by a straightforward extension of the present work; this is likely an absolute necessity for the reliable 3D simulation of bone cement infiltration of the trabecular skeleton.

Cement rheology is probably the most important factor for injection. Cement viscosity and curing rate may differ by orders of magnitude between different cements. The infiltration tests were carried out using one specific cement and only ten samples taken from two cadavers. However, the approach proposed here is generic, and therefore applicable to any kind of cement or polymer to be used for this procedure. Also, this approach can be used to examine a larger porosity range than the range examined in this study.

This study is the first to analyze cement flow through osteoporotic bone. The theoretical and experimental models provided in this paper are generic, and thus can be used to systematically study and optimize the infiltration process for clinical practice.

The significance of the theoretical and experimental models proposed here extends far beyond a vertebroplasty or one specific biomaterial. Fragility fractures in osteoporotic bone are mainly observed in the spine, proximal femur, and wrist. Cement augmentation is a measure not only to stabilize or prevent fragility fractures, but also

to anchor osteosynthesis materials in osteoporotic bone. The experimental and theoretical models presented in this paper are equally applicable to the proximal femur and wrist for preventative as well as palliative treatments. Furthermore, the use of computer mechanics (infiltration simulation) based on the current experimental and theoretical models gives us an interesting opportunity to investigate more realistically cement infiltration through osteoporotic bone.

Acknowledgements

This work has been supported by the Canadian Institute of Health Research (CIHR) Grant Number MOP 57835.

The cement used in this study was sponsored by Stryker Canada Inc. No other benefits were received or will be received from a commercial party related directly or indirectly to this article.

References

- [1] Riggs BL, Melton LJ. The worldwide problem of osteoporosis: insights afforded by epidemiology. *Bone* 1995;17(5):505S–511S.
- [2] Cotton A, Boutry N et al. Percutaneous vertebroplasty: state of the art. *Radiographics* 1998;18(2):311–20.
- [3] Heini PF, Walchli B et al. Percutaneous transpedicular vertebroplasty with PMMA: operative technique and early results. A prospective study for the treatment of osteoporotic compression fractures. *Eur Spine J* 2000;9(5):445–50.
- [4] Mathis JM, Barr JD et al. Percutaneous vertebroplasty: a developing standard of care for vertebral compression fractures. *AJNR Am J Neuroradiol* 2001;22(2):373–81.
- [5] Jensen ME, Evans AJ et al. Percutaneous polymethylmethacrylate vertebroplasty in the treatment of osteoporotic vertebral body compression fractures: technical aspects. *AJNR Am J Neuroradiol* 1997;18(10):1897–904.
- [6] Krause WR, Miller J et al. The viscosity of acrylic bone cements. *J Biomed Mater Res* 1982;16(3):219–43.
- [7] Baroud G, Falk R et al. Constitutive model and parameter identification for the cement infiltration of osteoporotic bone. 10th Annual Symposium On Computational Methods in Orthopaedic Biomechanics. Dallas, TX, 2002, p. 21.
- [8] Mazess RB, Gifford CA et al. DEXA measurement of spine density in the lateral projection. I: Methodology. *Calcif Tissue Int* 1991;49(4):235–9.
- [9] Beaudoin AJ, Mihalko WM et al. Finite element modelling of polymethylmethacrylate flow through cancellous bone. *J Biomech* 1991;24(2):127–36.
- [10] Grimm MJ, Williams JL. Measurements of permeability in human calcaneal trabecular bone. *J Biomech*. 1997;30(7):743–5.
- [11] Peh WCG, Gilula LA et al. Percutaneous vertebroplasty for severe osteoporotic vertebral body compression fractures. *Radiology* 2002;223(1):121–6.